Sismabeton: a new frontier for ductile concrete

Bernardino Chiaia, Alessandro P. Fantilli, Paolo Vallini
Politecnico di Torino, Dep. of Structural and Geotechnical Engineering Corso Duca degli Abruzzi, 24 -10129 Torino, Italy
fantilli@polito.it, vallini@polito.it, chiaia@polito.it

RIASSUNTO. I calcestruzzi fibrorinforzati ed autocompattanti (definiti Sismabeton) manifestano una elevata duttilità non solo in trazione ma anche in presenza di sforzi compressione. Ciò e messo in evidenza nel presente lavoro attraverso la misura della risposta meccanica, in regime di compressione triassiale, di calcestruzzi ordinari (NC) ed autocompattanti (SC) con e senza fibre. In strutture semplicemente compresse, la presenza del Sismabeton è da sola sufficiente a garantire un confinamento attivo uniforme.

ABSTRACT. The high ductility of Fiber Reinforced Self-consolidating concrete (called Sismabeton) can be developed not only in tension but also in compression. This aspect is evidenced in the present paper by measuring the mechanical response of normal concrete (NC), plain self-compacting concrete (SC) and Sismabeton cylindrical specimens under uniaxial and triaxial compression. The post-peak behaviour of these specimens is defined by a non-dimensional function that relates the inelastic displacement and the relative stress during softening. Both for NC and SC, the increase of the fracture toughness with the confinement stress is observed. Conversely, Sismabeton shows, even in absence of confinement, practically the same ductility measured in normal and self-compacting concretes with a confining pressure. Thus, the presence of Sismabeton in compressed columns is itself sufficient to create a sort of active distributed confinement.

KEYWORDS. Fiber-reinforced concrete, self-compacting concrete, confining pressure, triaxial tests, fracture toughness.

INTRODUCTION

Several reinforced concrete (RC) structures fail via concrete crushing in compressed zones. This is the case, for instance, of over-reinforced concrete beams, like those in four point bending tested by Mansur et al. [1]. When fiber-reinforced, the post-peak behaviour of such members is remarkably more ductile than that observed in beams having the same geometry, the same steel rebars, and the same bearing capacities, but made of normal concrete (NC) without fiber. Thus, when crushing occurs, the type of concrete rules both the mechanical response and the ductility of RC structures.

The experimental campaign conducted by Khayat et al. [2] on highly confined RC columns, subject to concentric compression, also confirms the influence of the cement-based composites on the structural performances. More precisely, for a given cross-section, the load *vs.* average axial strain diagrams appear more ductile in the case of columns made of self-compacting concrete (SC) than in NC columns.

These experimental observations can be usefully applied to designing RC compressed columns in seismic regions. According to Eurocode 8 [3], if a required ductility cannot be attained because concrete strains are larger than 0.35%, a compensation for the loss of resistance due to crushing can be achieved by means of an adequate confinement.

Such a confinement, usually provided by transversal steel reinforcement (i.e., stirrups), and indicated by the confining pressure σ_3 (Fig.1), allows designers to consider a more ductile stress strain (σ_c-ε_c) relationship in compression. For instance, Fig.1 shows the so-called parabola-rectangle diagrams proposed by Eurocode 2 [4] for confined and unconfined concretes.

Short steel fibers randomly dispersed in a cement-based matrix can generate confining pressures comparable with that of stirrups. The experimental campaign of Ganesan and Ramana Murthy [5], performed on short confined columns with and without fibers (Fig.2a), investigates on this aspect. As shown in Fig.2b, the applied load- average strain (P-ε_{cm}) diagram of RC columns, made with ordinary concrete and a transversal reinforcement percentage equal to ρ_s=1.6%, is more or less similar (in terms of strength and ductility) to that of fiber-reinforced (FRC) columns, made with a reduced quantity of stirrups (ρ_s =0.6%) and FRC (volume fraction V_f = 1.5%, aspect ratio L/Φ = 70).

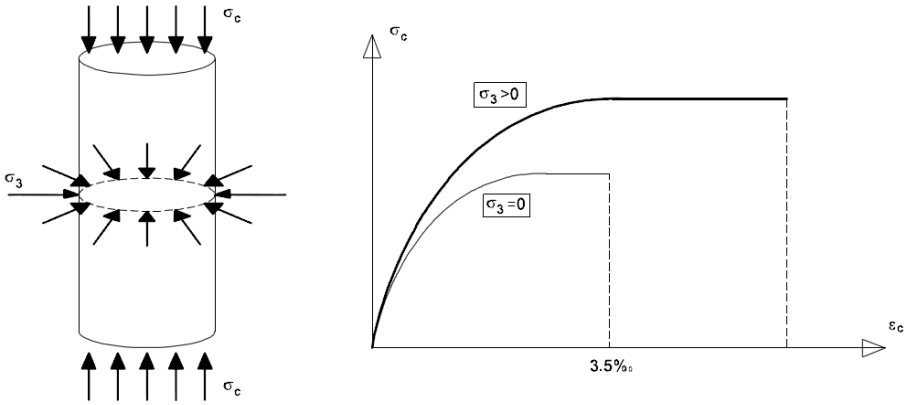

Figure 1: The stress-strain relationship of compressed concrete with and without confinement [4].

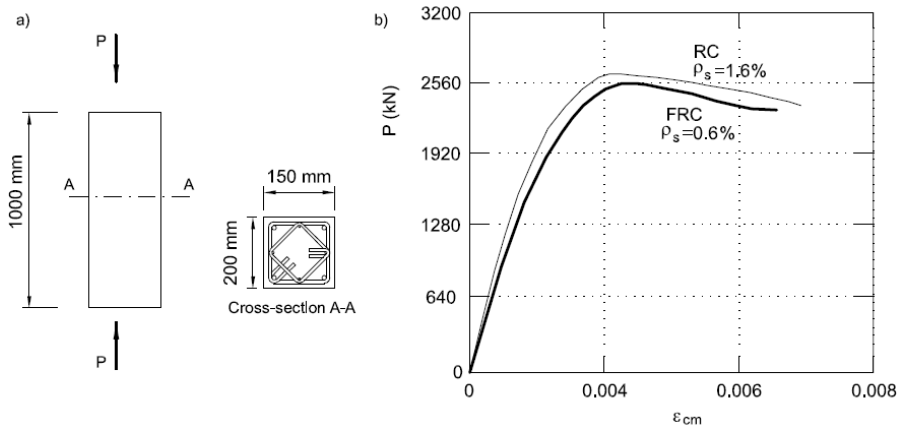

Figure 2: The columns tested by Ganesan and Ramana Murthy [5].

Although fiber-reinforcements have been introduced in order to increase the ductility of cement-based composites in tension, they can also provide a sort of confinement, and therefore higher ductility in compression. For this reason, when a better fiber matrix bond can be achieved, like the Fiber-Reinforced Self-compacting Composites [6], higher compressive fracture toughness should be expected. To confirm such a conjecture, the post-peak responses of different cementitious composites under uniaxial and multi-axial compression are here investigated.

POST-PEAK RESPONSE OF CONCRETE UNDER COMPRESSION

The stress-strain relationships of concrete and quasi-brittle materials in compression (Fig.3a) can be divided into two parts (Fig.3b). In the first part, when the stress is lower than the strength f_c (and $\varepsilon_c < \varepsilon_{c1}$), the specimen can be considered undamaged. In the case of plain concrete, the ascending branch of σ_c-ε_c can be defined by the Sargin's relationship proposed by CEB-FIP Model Code [7]. As soon as the peak stress is reached, localized damage develops and strain softening begins. In this stage, the progressive sliding of two blocks of the cement-based material is evident. In Fig.3a, the angle between the vertical axis of the specimen and the sliding surfaces is assumed to be α=18°. This value, as measured in many tests, can be also obtained through the Mohr-Coulomb failure criterion, if the tensile strength is

assumed to be 1/10 of compression strength ($f_{ct} = 0.1\ f_c$). The inelastic displacement w of the specimen, and the consequent sliding s of the blocks along the sliding surface, are the parameters governing the average post-peak compressive strain ε_c of the specimen (Fig. 3).
Referring to the specimen depicted in Fig. 3a, post peak strains can be defined by the following equation [8]:

$$\varepsilon_c = \varepsilon_{c,el} + \frac{w}{H} = \varepsilon_{c1} - \frac{\Delta\sigma_c}{E_c} + \frac{w}{H} \tag{1}$$

where, ε_{c1} = strain at compressive strength f_c; $\Delta\sigma_c$ = stress decrement after the peak; H = height of the specimen (see Fig. 1b).

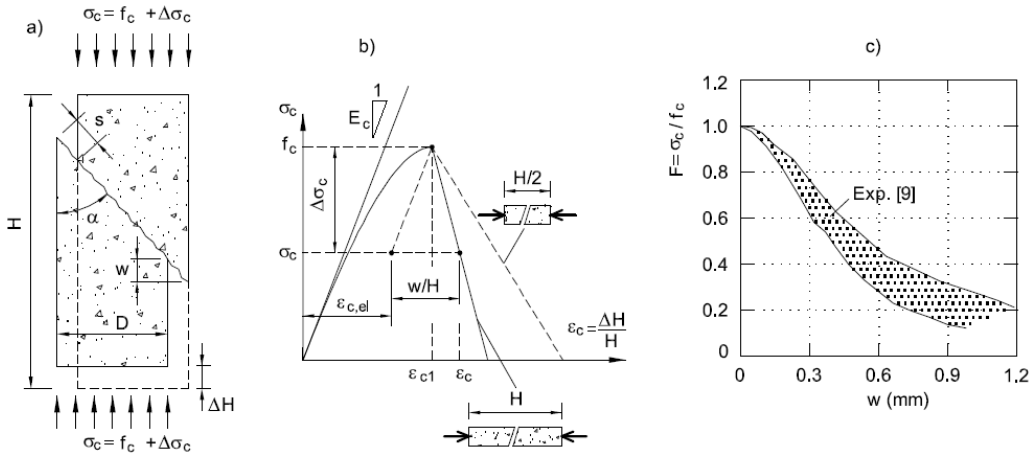

Figure 3: The post-peak response of quasi-brittle materials in compression.

According to test measurements [8, 9], the post-peak slope of σ_c-ε_c increases in longer specimens (Fig.3b), due to the w/H ratio involved in the evaluation of ε_c [Eq.(1)]. The stress decrement $\Delta\sigma_c$ can be defined as:

$$\Delta\sigma_c = f_c - \sigma_c = f_c \cdot \left[1 - F(w)\right] \tag{2}$$

where, $F(w)$ = non-dimensional function which relates the inelastic displacement w and the relative stress σ_c / f_c during softening (Fig.3c); f_c = compressive strength (assumed to be positive).
Substituting Eq.(2) into Eq.(1), it is possible to obtain a new equation for ε_c:

$$\varepsilon_c = \varepsilon_{c1} - \frac{f_c \cdot \left[1 - F(w)\right]}{E_c} + \frac{w}{H} \qquad \text{for} \quad \varepsilon_c > \varepsilon_{c1} \tag{3}$$

Eq.(3), adopted for the post-peak stage of a generic cement-based material in compression, is based on the definition of $F(w)$, which has to be considered as a material property [8-9]. In all cement-based composites, this function should be evaluated experimentally on cylindrical specimens, as performed by Jansen and Shah [9] for plain concrete (Fig.3c).
Fig.4a shows the $F(w)$ relationships proposed by Fantilli et al. [10]. It consists of two parabolas and a constant branch:

$$F(w) = \frac{\sigma}{f_c} = 1 + a \cdot w^2 + b \cdot w \qquad \text{for} \quad 0 \le w \le -\frac{b}{2 \cdot a} \tag{4a}$$

$$F(w) = \frac{\sigma}{f_c} = -\left(1 - \frac{b^2}{4 \cdot a}\right) \cdot \left(\frac{4 \cdot a^2}{b^2} w^2 + \frac{4 \cdot a}{b} w\right) \qquad \text{for} \quad -\frac{b}{2 \cdot a} < w \le -\frac{b}{a} \tag{4b}$$

$$F(w) = \frac{\sigma}{f_c} = 0 \qquad \text{for} \quad w > -\frac{b}{a} \tag{4c}$$

The parabolas are both defined by the same coefficients a, b and have the same extreme point at $w = -0.5\ b/a$, whereas $w = -\ b/a$ (i.e. twice the value at extreme point) is considered the maximum inelastic displacement corresponding to $F(w)$ higher than zero.

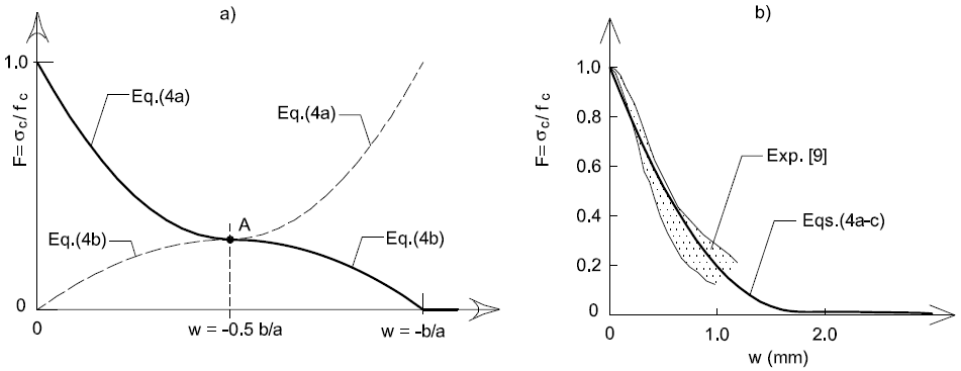

Figure 4: The stress-inelastic displacement relationship proposed by Fantilli et al. [10].

In the case of the plain concrete specimens, the values $a = 0.320$ mm^{-2} and $b = -1.12$ mm^{-1} were obtained by means of the least square approximation of several tests [10]. As observed in Fig.4b, the curves defined by Eqs.(4) fall within the range of the data experimentally measured by Jansen and Shah [9].

In the case of multi-axial compression, stress-inelastic displacement relationships, which should reproduce the confined post-peak stage, cannot be found in the existing literature. As is well known, two types of confinement, namely passive and active, can be produced. In compressed columns, passive confinements provided by transversal reinforcement (i.e., stirrups, tubes, strips, spirals, etc.), are only activated by concrete displacements. Thus, to define quantitatively this contribution, it is necessary to know the stress-transversal displacement relationship of concrete. Active confinement is due to external stresses σ_3 applied by multi-axial compression tests on cubes in two or three directions, or by triaxial tests on cylinders (see the book by van Mier [8] for a review).

Only a single campaign of triaxial tests, performed by Jamet et al. [11] on micro-concrete, is reported in the current literature. In that case, the applied confinement was relatively high ($\sigma_3 > 3$ MPa), if compared to those produced by stirrups in ordinary RC columns. In accordance with Eurocode 2 [4], in columns under concentric compression, transverse reinforcement can develop about $\sigma_3 = 1$MPa [12]. Consequently, with the aim of analyzing the equivalent confing pressures produced by a new Fiber-reinforced Self-consolidating concrete (called Sismabeton), the comparison between the results of new triaxial tests on NC, SC and Sismabeton cylinders under uniaxial compression are reported.

EXPERIMENTAL PROGRAM

The post-peak behaviour of cement-based composites under multi-axial compression has been investigated at the Department of Structural and Geotechnical Engineering of Politecnico di Torino (Italy) by means of triaxial tests on concrete cylinders (Fig.5a). The experimental equipment, named HTPA (High Pressure Triaxial Apparatus) and described by Chiaia et al. [13], is generally used to test cylindrical specimens made of soft rocks.

Each triaxial test consists of two stages. A specimen is initially loaded with a hydrostatic pressure σ_3 (Fig.5b), then deviatoric loads P are applied along the longitudinal direction with a velocity of 0.037 mm per minute (Fig.5c). During the second stage of loading, the confining pressure $\sigma_3 = const.$ is applied to the lateral surface, whereas the longitudinal nominal stress σ_c becomes:

$$\sigma_c = \sigma_3 + \frac{4P}{\pi D^2} \tag{5}$$

where, P = applied deviatoric load; D = diameter of the cross-section.

Through a couple of LVDT, local longitudinal displacements, and therefore nominal longitudinal strains ε_c, are also measured (Fig. 5a).

Two confining pressures, namely $\sigma_3 = 0$ MPa and $\sigma_3 = 1$ MPa (reached in 10 minutes), are applied to the specimens. During the application of hydrostatic loads (Fig.5b), stress increments are electronically recorded every 10 seconds.

Similarly, in the second stage, when σ_3 = *const.* and P increases, the values of deviatoric load, the relative displacement between the specimen's ends, and the longitudinal displacement along the lateral surface (taken by the LVDTs of Fig.5a) are measured.
Two types of self-consolidating concrete (SC_mix1 and SC_mix2) and a single ordinary concrete (NC) were tested.

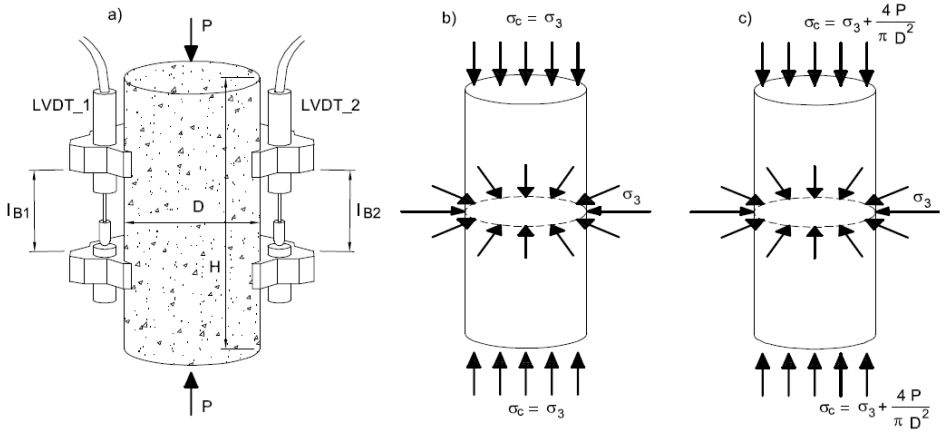

Figure 5: The two stages of triaxial tests on cement-based cylinders.

Their compositions and strengths are reported in Tab. 1. Specifically, the self-consolidating concretes have the same unit weight, but different amounts of aggregates. With respect to SC_mix1, in a cube meter of SC_mix2 the content of carbonate filler was increased by 90 N and, contemporarily, the weight of coarse aggregate was reduced by the same quantity.
Regarding the Fiber-reinforced Self-consolidated concrete (i.e., Simabeton), two specimens were tested, under uniaxial compression ($\sigma_3 = 0$). As indicated in Tab. 1, Sismabeton is reinforced with 700 N/m³ of Dramix RC 65/35 BN steel fibers having hooked ends (length L = 35 mm, diameter Φ = 0.55 mm, volume fraction V_f = 0.9%). which were added to the self-consolidating concrete with the higher quantity of filler (i.e., SC_mix2).

Component	NC N/m³	SC_mix 1 N/m³	SC_mix 2 N/m³	Sismabeton N/m³
Water	1770	1770	1770	1770
Superplasticizer (Addiment Compactcrete 39/T100)	-	44	44	44
Superplasticizer (Addiment Compactcrete 39/T11)	14	-	-	-
Cement (Buzzi Unicem II/A-LL 42.5 R)	2840	2450	2450	2450
Carbonate filler (Nicem Carb VG1-2)	0	3240	3730	3730
Fine aggregate (0-4 mm)	8830	8930	8930	8930
Coarse aggregate (6.3-12 mm)	6380	6380	5890	5890
Steel fibers Dramix RC 65/35 BN	-	-	-	700
Cubic strength -MPa-	30.0	31.1	30.4	33.8

Table 1: Compositions and strengths of NC, SC_mix1, SC_mix2, and Sismabeton.

The specimens of each concrete mixture were cast simultaneously in polystyrene form, then cured for one week under identical laboratory conditions, and finally tested after one month. Three couples of cylinders, with H=140 mm and D=70 mm, were made of NC (NC0 and NC1), SC_mix1 (SC0 and SC1), and SC_mix2 (SC0b and SC1b). The two specimens of

these couples were tested, respectively, at σ_3 = 0 MPa and σ_3 = 1 MPa. Two Sismabeton cylinders (HC0 and HC0b), with H=140 mm and D=70 mm, were tested in uniaxial compression. The properties of each specimen are reported in Tab. 2.

Specimen	H (mm)	D (mm)	Type of concrete	σ_3 (MPa)
NC0	140	70	NC	0
NC1	140	70	NC	1
SC0	140	70	SCC mix 1	0
SC1	140	70	SCC mix 1	1
SC0b	140	70	SCC mix 2	0
SC1b	140	70	SCC mix 2	1
HC0	100	50	Sismabeton	0
HC0b	100	50	Sismabeton	0

Table 2: Mechanical and geometrical properties of the specimens tested in uniaxial and triaxial compression.

TEST RESULTS

Fig. 6 reports the stress-strain relationships obtained from the specimens made respectively with Sismabeton (Fig.6a), normal concrete (Fig.6b) and self-consolidating concrete (Fig.6c). The higher the confinement, the higher the values of f_c and ε_{c1}, which are reported, together with Young's modulus E_c, in Tab. 3. In all the cases, after the peak stress f_c, a remarkable strain softening branch can be observed in the σ_c-ε_c diagrams.
Although Sismabeton is fiber-reinforced, its compressive strength does not differ substantially from those of ordinary and self-consolidating concrete. However, the post peak response of Sismabeton appears more ductile. Only when the confining pressure σ_3 increases, does the ductility of NC and SC increase. By comparing all the post-peak branches reported in Fig.6, it seems that the post-peak branches of SC and NC specimens in the presence of σ_3=1 MPa are more or less the same of Sismabeton without any confinement.

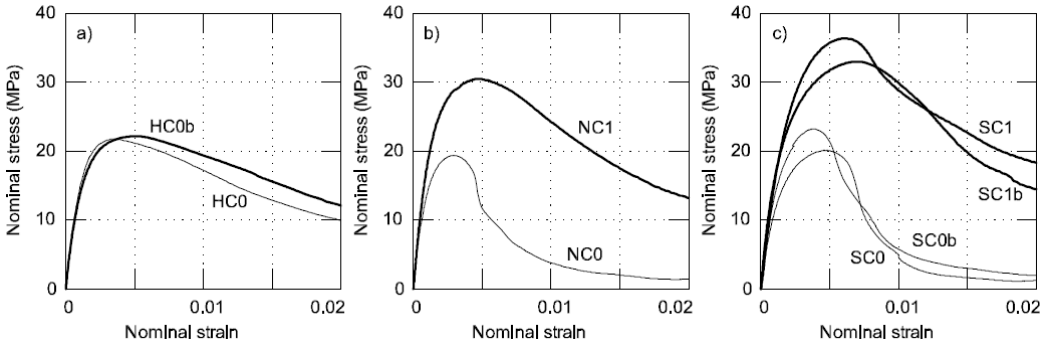

Figure 6: The stress-strain relationships of Sismabeton, NC and SC.

Specimen	f_c (MPa)	ε_{c1} (%)	E_c (MPa)
0NC0	19.4	0.293	24000
0NC1	30.5	0.473	23000
0SC0	20.1	0.479	17000
0SC0b	23.2	0.372	23000
0SC1	36.4	0.604	19000
0SC1b	32.0	0.696	27000
HC0	21.8	0.352	19000
HC0b	22.2	0.534	20000

Table 3: Mechanical properties measured in the tests.

However, a direct comparison between the analyzed concretes is not possible in terms of nominal stress and strain, because specimens have different nominal strengths.

Post-peak comparison in terms of F(w)

A more accurate comparison between the post-peak responses of Sismabeton, NC and SC under compression can be conducted in terms of $F(w)$ (Fig.7). In particular, for a given $\varepsilon_c > \varepsilon_{c1}$, the decrease of compressive stress $\Delta\sigma_c = f_c - \sigma_c$ (and $F = \sigma_c / f_c$) can be obtained through the σ_c-ε_c diagrams experimentally evaluated (Fig.6), whereas the corresponding w (Fig.3a) can be obtained from Eq.(3) (f_c , ε_{c1} , E_c and H are known from the tests).

The $F(w)$ curves reported in Fig.7 are limited to w = 2mm, when compressive strains ε_c are relatively high although, in some cases, stresses are higher than zero. However, in all the tests the relative stress $F = \sigma_c / f_c$ decreases with w. The dashed curves reported in Fig.7 represent the behaviour of NC and SC as predicted by Eq.(4) in the case of zero confinement. As in the case of $\sigma_3 = 0$ the post-peak responses of the specimens NC0, SC0, SC0b are correctly predicted by Eq.(4), and all the tests can be considered consistent [10].

Both for NC and SC, Fig.7a and Fig7b, respectively show the increase of the compressive fracture toughness (within the range w~0-2 mm) with the confining pressure σ_3. However, this phenomenon is also evident in the case of Sismabeton, which can show, in absence of confinement, more or less the same $F(w)$ obtained for NC and SC when σ_3 = 1MPa.

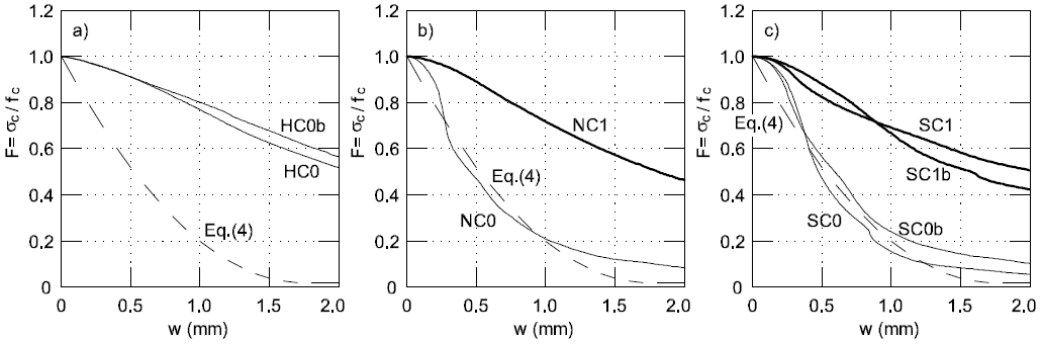

Figure 7: The post peak behaviour in terms of $F(w)$.

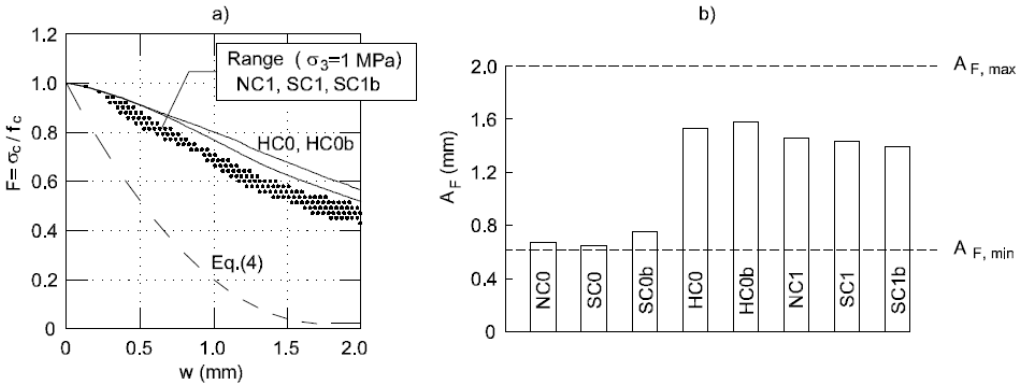

Figure 8: The active confinement of Sismabeton.

Fig.8a shows the post-peak responses of the specimens HC0 and HC0b, which are closer to those of confined SC and NC (i.e., the range defined by NC1, SC1, SC1b), than to the theoretical $F(w)$ obtained in absence of confinement [10] (the dashed line in Fig.8a).

Within the observed range (w~0-2 mm), compressive facture toughness of different concretes can be objectively measured by the area A_F under the function $F(w)$:

$$A_F = \int_0^2 F(w)\, dw \qquad (6)$$

In fact, as $F(w)$ is a relative stress normalized with respect to the compressive strength f_c, a comparison between all the cement-based composites, under uniaxial and multi-axial compression, is possible. Higher values of A_F are attained in concretes capable of maintaining high loads after failure (i.e., in the case of ductile materials). Obviously, the maximum ductility $A_{F,max}$ = 2mm is reached in the case of plastic behaviour [$F(w)$ = 1= *const.*].
The areas A_F computed by Eq.(6) for the tested specimens (Tab. 2) are also reported in the histogram of Fig. 8b. In all cases, A_F is between $A_{F,max}$ = 2 mm and the lower limit $A_{F,min}$ = 0.61 mm, corresponding to the normal and self-consolidating concretes without any confinement (Fig.8b). To be more precise, $A_{F,min}$ is obtained by substituting Eqs.(4) (with a = 0.320 mm^{-2} and b = -1.12 mm^{-1}) into Eq.(6). At σ_3 = 1MPa, for the specimens made of SC and NC (i.e., NC1, SC1, SC1b) the values of A_F range between 1.39 mm and 1.46 mm (Fig.8b), and do not differ substantially from those measured for Sismabeton ($A_F \cong$1.56 mm) without confinement.

CONCLUSIONS

From the results of an experimental campaign performed on NC, SC and Sismabeton cylinders under uniaxial and multi-axial compression, the following conclusion can be drawn:

- In normal and self-consolidating concrete, fracture toughness in compression increases in the presence of an active confinement.
- During the post-peak stage, the ductility of Sismabeton is comparable with that of NC or SC at 1MPa of confining pressure.
- In compression, the performance of fiber-reinforced composites can be quantified by the distributed confining pressure generated by the fibers.

The presence of an active confinement can improve the mechanical behaviour of concrete and, consequently, its durability. Thus, further researches should be developed in order to introduce new sustainability indexes, which take into account fracture toughness, both in tension and compression.

ACKNOWLEDGEMENTS

The authors wish to express their gratitude to the Italian Ministry of University and Research (PRIN 2006) and to Fondazione Cassa di Risparmio di Alessandria for financing this research work, and also to Buzzi Unicem S.p.A. for its technical support.

REFERENCES

[1] M. A. Mansur, M. S. Chin, T. H. Wee, ACI Structural Journal, 94-6 (1997) 663.
[2] K. H. Khayat, P. Paultre, S. Tremblay, ACI Materials Journal, 98-1 (2001) 371.
[3] UNI EN 1998-1:2005. Eurocodice 8 – Design of structures for earthquake resistance - Part 1: General rules, seismic actions and rules for buildings, (1998) 229
[4] UNI EN 1992-1-1:2005. Eurocodice 2- Design of concrete structures- Part 1-1: General rules and rules for building, (1992) 225.
[5] N. Ganesan, J. V. Ramana Murthy, ACI Materials Journal, 87-3 (1990) 221.
[6] G. Pons, M. Mouret, M. Alcantara, J. L. Granju, Materials and Structures, 40-2 (2007) 201.
[7] CEB (Comite Euro-International du Beton), "CEB-FIP Model Code 1990", bulletin d'information n°203-205, Thomas Telford, London, UK (1993).
[8] J. G. M. van Mier, , Fracture Processes of Concrete: Assessment of Material Parameters for Fracture Models. CRC Press, (1996) 448.
[9] D. C. Jansen, S. P. Shah, ASCE Journal of Engineering Mechanics, 123-1 (1997) 25.
[10] A. P. Fantilli, H. Mihashi, P. Vallini, ACI Materials Journal, 104-5 (2007) 501.
[11] P. Jamet, A. Millard, G. Nahas, Int. conference on concrete under multiaxial conditions, Toulouse (1984) 133.
[12] S. J. Foster, J. Liu, S. A. Sheikh, ASCE Journal of Structural Engineering, 124-12 (1998) 1431.

[13] B. Chiaia, A. P. Fantilli, P. Vallini, in 3rd North American Conference on the Design and Use of Self-Consolidating Concrete (SCC), Chicago (2008).